Electronic Mode Stirring for Reverberation Chambers

David A. Hill, *Fellow, IEEE*

Abstract—**A modal analysis and a uniform-field approximation are presented for the fields in an idealized two-dimensional, rectangular cavity excited by an electric line source. The model is used to evaluate the effectiveness of frequency stirring, an alternative to mechanical stirring in reverberation chamber immunity measurements. Numerical results indicate that good field uniformity (standard deviation less than 1 dB) can be obtained with a bandwidth of 10 MHz at a center frequency of 4 GHz. The bandwidth requirement is determined primarily by the number of modes excited, and higher frequencies can achieve the same field uniformity with a smaller bandwidth because of the higher mode density. Cavity excitation by two single-frequency sources is also analyzed.**

I. Introduction

REVERBERATION chambers (also called mode-stirred or mode-tuned chambers) [1]–[5] are becoming increasingly popular for electromagnetic immunity testing. Such chambers can generate high field strengths using modest power sources. The goal of reverberation chambers is to create a statistically uniform field that eliminates the need to rotate the test object.

A mechanical mode stirrer (paddle wheel) is usually used to vary the chamber boundary conditions in an attempt to obtain statistical field uniformity. Mechanical stirring can be quite effective [4], but it is fairly slow. In their analysis of mechanical stirring, Wu and Chang [6] pointed out that the rotating mechanical stirrer continuously changes the resonant frequencies of the cavity modes and that mechanical stirring has some equivalence to frequency modulation of the source.

Loughry [7] made statistical predictions of the field homogeneity achieved by frequency stirring and performed comparison measurements using a band-limited, white, Gaussian noise source. In this paper, the Green's function for a two-dimensional, rectangular cavity is used to perform field uniformity calculations as a function of the source bandwidth and cavity parameters. The two-dimensional model is idealized, but it contains most of the relevant physics of the problem and was shown to be useful in an analysis of mechanical stirring [6].

The organization of this paper is as follows. In Section II two expressions for the Green's function for a line source in a perfectly conducting, rectangular cavity are derived. An approximate Green's function is also obtained for the case of a lossy cavity in terms of the quality factor (Q) of the cavity. In Section III, Dunn's method [8] is used to derive an expression for the cavity Q. An approximate expression is also derived for the power density in the cavity by using a uniform power density assumption of the type used in room acoustics [9]. In Section IV, the frequency bandwidth of a single line source is varied, and spatial field uniformity is computed for a variety of cases. In Section V, the use of two single-frequency sources with variable phase for exciting the cavity is analyzed. This method has practical significance for high-power excitation, but the phase stirring by itself does not produce good field uniformity. Conclusions and recommendations are given in Section VI.

Manuscript received July 28, 1993; revised April 23, 1994.
The author is with the Electromagnetic Fields Division, National Institute of Standards and Technology, Boulder, CO 80303 USA.
IEEE Log Number 9404488.

Fig. 1. Geometry for an electric line source in a two-dimensional, rectangular cavity.

II. Green's Function

The geometry for an electric line source of current I_0 located at (x_0, y_0) in a two-dimensional rectangular cavity ($a \times b$) is shown in Fig. 1. The cavity region has free-space permittivity ϵ_0 and permeability μ_0. Initially, the cavity walls are are assumed to be perfect electric conductors so that the tangential electric field is zero at the cavity walls.

The fields are independent of z ($\partial/\partial z = 0$) and have $\exp(j\omega t)$ time dependence. For a real, three-dimensional cavity ($a \times b \times c$), a realistic source will excite additional modes with z variation not included in this analysis. However, a line source with no z variation ($\partial/\partial z = 0$) over the cavity dimension c would excite only the modes considered in this two-dimensional model.

The nonzero field components are E_z, H_x, and H_y, and the magnetic field components can be derived from the z-directed electric field E_z

$$H_x = \frac{1}{j\omega\mu_0}\frac{\partial E_z}{\partial y} \quad \text{and} \quad H_y = \frac{-1}{j\omega\mu_0}\frac{\partial E_z}{\partial x}. \tag{1}$$

The Green's function (for E_z) must satisfy the following scalar equation:

$$\left(\frac{\partial^2}{\partial x^2} + \frac{\partial^2}{\partial y^2} + k^2\right)E_z = j\omega\mu_0 I_0 \delta(x - x_0)\delta(y - y_0) \tag{2}$$

where $k^2 = \omega^2\mu_0\epsilon_0$ and δ is the Dirac delta function. (E_z is used rather than the usual G notation for the Green's function because there is no need to integrate over an extended source region to obtain the electric field E_z.) To make the solution of (2) for E_z unique, the condition that $E_z = 0$ is enforced at the cavity boundaries.

Using standard separation of variables techniques [10], (2) can be solved for E_z in the following double summation form (see (3) at the bottom of the page). The denominator of (3) has zeros at cavity resonant frequencies f_{mn} given by

$$f_{mn} = (c/2)[(m/a)^2 + (n/b)^2]^{1/2} \quad (4)$$

where the speed of light $c = 1/(\mu_0\epsilon_0)^{1/2}$ and m and n run over all positive integers. The solution in (3) includes only sine terms that satisfy the boundary condition at the cavity walls on a term-by-term basis.

It is possible to sum the n summation (or the m summation) in (3) and obtain the following alternative expression [10] for E_z:

$$E_z = \frac{-2j\omega\mu_0 I_0}{a}\sum_{m=1}^{\infty}\frac{\sin(m\pi x_0/a)\sin(m\pi x/a)}{k_m \sin(k_m b)} \times \begin{cases}\sin(k_m y_0)\sin[k_m(b-y)], & y > y_0\\ \sin[k_m(b-y_0)]\sin(k_m y), & y < y_0\end{cases} \quad (5)$$

where

$$k_m = [k^2 - (m\pi/a)^2]^{1/2}.$$

Both (3) and (5) agree with the related scalar Green's function in [10].

Because (3) and (5) apply to a lossless cavity with perfectly conducting walls, they have singularities at the resonant frequencies given by (4). No exact solution exists for the physically realistic case of lossy walls, but (3) and (5) can be modified in a simple way to obtain a fairly accurate solution for the case of fairly high Q. There are several slightly different forms for the finite Q modification, but for large Q they are approximately equivalent. Here loss is introduced by replacing k in (3) and (5) by the following complex k_c [10]–[15]:

$$k_c = k\left(1 - \frac{j}{2Q}\right). \quad (6)$$

In the following section, an expression for Q will be derived based on wall loss. However, other loss mechanisms can lead to a finite Q [16], and (6) can also represent other types of loss. For example, if the cavity filling is a dielectric with loss, then (6) actually represents the wavenumber of the dielectric [14], [15].

For computational efficiency, the expression in (5) is preferred because it involves only a single sum. The sum is finite for finite Q because k_m becomes complex with the substitution indicated in (6)

$$k_m = \left[k^2\left(1 - \frac{j}{2Q}\right)^2 - (m\pi/a)^2\right]^{1/2}. \quad (7)$$

Thus both k_m and $\sin(k_m b)$ are nonzero for all real frequencies so that (5) remains finite. An examination of the denominator of (3) indicates that the 3-dB bandwidth of any given mode is approximately f_{mn}/Q, where f_{mn} is given by (4). Computer programs have been written to evaluate E_z from both (3) and (5), and they have been shown to agree numerically. However, the program based on (5) is much faster because it is a single sum and because the terms decay exponentially for $m > ka/\pi$. This greater computational speed is important in Section IV where repeated calculations are performed for many frequencies and observation points.

III. Uniform-Field Approximations

Before performing field calculations from the mode theory of the previous section, approximate expressions are developed for the cavity Q and power density based on the statistically uniform field approximation used in room acoustics [9] and in mode-stirred chambers [8]. The first assumption is that the line source radiates the same power in the lossy cavity that it does in a free-space environment. If (2) is solved for E_z using the radiation condition rather than a cavity wall boundary condition, then the expression for E_z is [15]

$$E_z = -\frac{\omega\mu_0 I_0}{4} H_0^{(2)}(k\rho) \quad (8)$$

where $\rho = (x^2 + y^2)^{1/2}$ and $H_0^{(2)}$ is the zero-order Hankel function of the second kind [17]. If the asymptotic expression for $H_0^{(2)}(k\rho)$ for large $k\rho$ is used, then the radiated power density S_r per unit length is

$$S_r = |E_z|^2/\eta_0 = \frac{|I_0|^2\eta_0 k}{8\pi\rho} \quad (9)$$

where $\eta_0 = (\mu_0/\epsilon_0)^{1/2}$. The power radiated per unit length P_r is obtained by multiplying S_r by the circumference $2\pi\rho$

$$P_r = 2\pi\rho S_r = |I_0|^2\eta_0 k/4. \quad (10)$$

The second assumption is that for a well-stirred cavity the power density $S(= |E_z|^2/\eta_0)$ and the energy density $W(= \eta_0|E_z|^2)$ are uniform throughout the cavity. By conservation of power, the power radiated must equal the power dissipated in the cavity and Q can be written

$$Q = \omega U/P_r \quad (11)$$

where U is the stored energy per unit length in the cavity. U can be written

$$U = WA = \epsilon_0|E_z|^2 A \quad (12)$$

where the cross-sectional area $A = ab$. In deriving (12) the stored electric and magnetic energies are assumed to be equal. This equality holds for a lossless cavity [15] and holds approximately for a high-Q cavity. By substituting (10) and (11) into (12), the square of the electric field is found to be

$$|E_z|^2 = |I_0|^2\eta_0^2 Q/(4ab). \quad (13)$$

$$E_z = \frac{4j\omega\mu_0 I_0}{ab}\sum_{m=1}^{\infty}\sum_{n=1}^{\infty}\frac{\sin(m\pi x_0/a)\sin(m\pi x/a)\sin(n\pi y_0/b)\sin(n\pi y/b)}{k^2 - (m\pi/a)^2 - (n\pi/b)^2}. \quad (3)$$

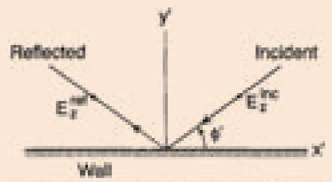

Fig. 2. Geometry for a single plane wave incident on a cavity wall.

The approximation in (13) is expected to hold only in some average sense where the fields are well-stirred. Even then, it cannot hold near the source and the cavity walls.

The missing piece of information in (13) is the cavity Q. In general, it is difficult to calculate Q because it is difficult to account for all the cavity losses [4]. However, Dunn's method [8] can be used to derive an expression for the two-dimensional cavity in terms of the wall conductivity σ_w and permeability μ_w. Consider a primed coordinate system where one of the walls interfaces is the $y' = 0$ surface as shown in Fig. 2. The total field is assumed to be a uniformly distributed ensemble of locally plane waves. A single plane wave with elevation angle ϕ' is shown in Fig. 2. Only E_z polarization is considered since only electric line source excitation is analyzed.

The incident electric field E_z^{inc} can be written

$$E_z^{inc} = E_0 \exp[jk(x' \cos\phi' + y' \sin\phi')] \tag{14}$$

where E_0 is a constant. For a highly conducting wall, the reflection coefficient is assumed to be -1. Then the total (incident plus reflected) electric field E_z is

$$E_z = E_0 \exp(jkx' \cos\phi') \times [\exp(-jky' \sin\phi') - \exp(jky' \sin\phi')]. \tag{15}$$

The corresponding squares of the magnitudes of the electric and magnetic field components are

$$\begin{aligned} |E_z|^2 &= 4|E_0|^2 \sin^2(ky' \sin\phi') \\ |H_{x'}|^2 &= (4/\eta_0^2)|E_0|^2 \sin^2\phi' \cos^2(ky' \sin\phi') \\ |H_{y'}|^2 &= (4/\eta_0^2)|E_0|^2 \cos^2\phi' \sin^2(ky' \sin\phi'). \end{aligned} \tag{16}$$

Ensemble averages over incidence angle ϕ' are defined in the form

$$\langle f(\phi') \rangle = \frac{1}{\pi} \int_0^{\pi} f(\phi')\, d\phi' \tag{17}$$

where f is an arbitrary function. Away from the interface (large ky'), the average values of the squared field components in (16) simplify to

$$\langle |E_z|^2 \rangle = 2|E_0|^2 \quad \text{and} \quad \langle |H_{x'}|^2 \rangle = \langle |H_{y'}|^2 \rangle = |E_0|^2/\eta_0^2. \tag{18}$$

The energy density W and stored energy U per unit length can both be written in terms of E_0

$$W = \epsilon_0 \langle |E_z|^2 \rangle = 2\epsilon_0 |E_0|^2 \quad \text{and} \quad U = WA = 2\epsilon_0 |E_0|^2 A. \tag{19}$$

The power dissipated P_A per unit area is [8]

$$P_A = \frac{\omega \mu_w \delta}{2} \langle |H_{tan}|^2 \rangle \tag{20}$$

where the skin depth $\delta = [2/(\omega \mu_w \sigma_w)]^{1/2}$. The average of the squared tangential magnetic field is

$$\langle |H_{tan}|^2 \rangle = \langle |H_x|^2 \rangle |_{y'=0} = 2|E_0|^2/\eta_0^2. \tag{21}$$

Substituting (21) into (20) and multiplying by the cavity perimeter L, the power dissipated P_L per unit length is

$$P_L = \omega \mu_r \delta \epsilon_0 |E_0|^2 L \tag{22}$$

where $\mu_r = \mu_w/\mu_0$ and $L = 2(a + b)$. Using (19) and (22), the final expression for Q can be written

$$Q = \omega U / P_L = \frac{2A}{\mu_r \delta L}. \tag{23}$$

IV. Frequency Stirring

If E_z (or H_x or H_y) is computed from (5), rapid variations are found with x and y due to standing waves or with frequency due to the mode structure. The mode density [2] is an important quantity in understanding the frequency behavior of fields in cavities. The mode density expression for a three-dimensional cavity is well known [2], but here the expression for a two-dimensional cavity is needed. Examining (4) shows that the number N of modes with resonant frequency less than f is approximately

$$N = \pi a b f^2 / c^2. \tag{24}$$

The mode density is the derivative of the mode number with respect to frequency

$$\frac{dN}{df} = 2\pi a b f / c^2. \tag{25}$$

The specific mode density N_s has been defined as the number of modes within the 3-dB bandwidth f/Q resulting from a finite Q [13]

$$N_s = \frac{f}{Q}\frac{dN}{df} = \frac{2\pi a b f^2}{Qc^2}. \tag{26}$$

Typically, the bandwidth f/Q is not large enough to bring in a significant number of modes to provide a uniform field through mode mixing. Mechanical mode stirring changes the resonant frequencies sufficiently to provide a well-stirred field [4], [6].

If the source has nonzero bandwidth BW, then the number of modes N_{BW} excited is

$$N_{BW} = 2\pi a b f BW / c^2. \tag{27}$$

This assumes that BW is somewhat greater than f/Q, but this is required in order to gain any advantage from the nonzero bandwidth. There is some freedom in the type of signal that is actually used to obtain the bandwidth, and Loughry [7] chose to use band-limited, white, Gaussian noise. Here the source spectrum is assumed flat over the bandwidth BW, and the field contributions from any two unequal frequencies are assumed orthogonal. (These assumptions are consistent with Loughry's source.)

Then the mean square field at any point can be written

$$|E_z|^2 = \frac{1}{BW} \int_{f-BW/2}^{f+BW/2} |E_z(f')|^2\, df'. \tag{28}$$

TABLE I
AVERAGE AND STANDARD DEVIATION OF THE FIELD AND THE NUMBER OF MODES EXCITED FOR VARIOUS BANDWIDTHS

f (GHz)	BW (MHz)	Q	y (m)	Aver. (dB)	Stand. Dev. (dB)	N_{BW}
4	0.0	1.0×10^5	1.5	-5.81	6.20	0.0
4	1.0	1.0×10^5	1.5	-4.90	3.04	3.9
4	5.0	1.0×10^5	1.5	-1.95	1.54	19.5
4	10.0	1.0×10^5	1.5	0.49	0.88	38.9
4	10.0	1.0×10^5	1.0	0.76	0.72	38.9
4	10.0	1.0×10^5	2.0	0.71	0.89	38.9
4	10.0	5.0×10^4	1.5	0.46	0.98	38.9
4	10.0	2.0×10^5	1.5	0.51	0.85	38.9
8	0.0	1.5×10^5	1.5	-4.83	5.13	0.0
8	1.0	1.5×10^5	1.5	2.04	2.69	7.8
8	5.0	1.5×10^5	1.5	0.30	1.27	38.9

If perfect field uniformity were achieved and if the line source were to radiate the same power that it would in a free-space environment, then (28) would agree with (13) at all points within the cavity. This suggests that (13) be used to normalize (28) to the ideal case and to compute a normalized field given by

$$|E_{zn}|^2 = \frac{1}{C_n^2 BW} \int_{f-BW/2}^{f+BW/2} |E_z(f')|^2 \, df'$$

where

$$C_n^2 = |I_0|^2 \eta_0^2 Q/(4ab). \tag{29}$$

The purpose of the following calculations is to see how closely the ideal case ($|E_{zn}|^2 = 1$) is approached as BW is increased.

In Figs. 3–6, the normalized electric field (in decibels) is shown as a function of x for a fixed value of y. For cavity dimensions, two dimensions from the NIST chamber [4] are chosen: $a = 4.57$ m and $b = 3.05$ m. The source location is fixed at $x_0 = y_0 = 0.5$ m. This is consistent with the practice of placing the transmitting antenna in one of the chamber corners, but not too close to the walls. The remaining parameters for Fig. 3 are $f = 4$ GHz, $Q = 10^5$, and $y = 1.5$ m. The Q value was selected to match the experimental value for the NIST chamber [4]. Two trends are clear as the bandwidth is increased in Fig. 3. The field variability as a function of x decreases, and the average field approaches 0 dB. This means that frequency stirring is effective both in improving spatial uniformity of the field and in reducing the interaction between the line source and the chamber walls. The second effect is equivalent to providing a free-space environment for the transmitting antenna, thus reducing impedance mismatch effects. The average value and the standard deviation of the normalized field and the number of modes excited are given in Table I for each curve in Figs. 3–6. The number of modes, as determined from (27), is not necessarily an integer because (27) is an approximate asymptotic expression. If discrete mode counting had been used, as in [2], then the number of modes would have been an integer.

In Fig. 4 similar results are shown for a higher frequency of 8 GHz. An increase in Q to 1.5×10^5 reflects the usual increase in chamber Q with frequency [4]. Again, the field uniformity improves with increasing bandwidth, and the average value approaches 0 dB. Equation (27) shows that the number N_{BW} of modes excited is proportional to f_{BW} so that a smaller bandwidth is needed at higher frequencies. Table I shows that the number of modes N_{BW} is the significant quantity in determining field uniformity, and this is consistent with [7].

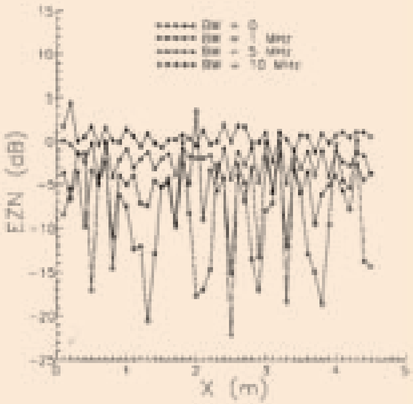

Fig. 3. Normalized electric field magnitude versus x for various bandwidths. Parameters: $f = 4$ GHz, $Q = 10^5$, $y = 1.5$ m, and $x_0 = y_0 = 0.5$ m.

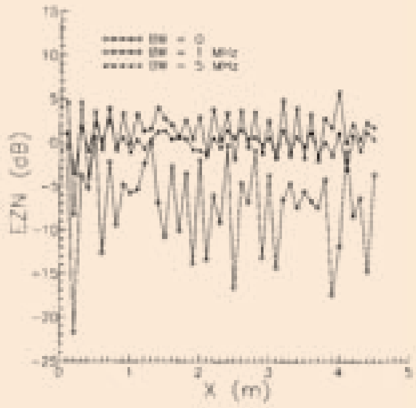

Fig. 4. Normalized electric field magnitude for a higher frequency (8 GHz) and Q (1.5×10^5).

In Fig. 5, results at 4 GHz are shown for three different y values. The three curves are quite distinct, but they have approximately the same statistics as seen in Table I. All three curves have average values and standard deviations less than 1 dB. This is a good illustration of the type of statistical spatial field uniformity that is to be expected with well-stirred fields in a reverberation chamber.

In Fig. 6 results are shown for three different Q values. In this case the actual curves, not just their statistics, are very similar. However, it should be remembered that the normalization in (29) involves Q. Thus the unnormalized field is higher for higher Q. Again, the average values and standard deviations are less than 1 dB for each case.

If the results of Table I are compared with Loughry's results, fewer modes are required to obtain a given level of field uniformity (for example, 1 dB) for the idealized two-dimensional model. This is to be expected since more modes are required to mix the fields in a fully three-dimensional cavity. If this factor is taken into account, then the results in Table I are consistent with Loughry's results.

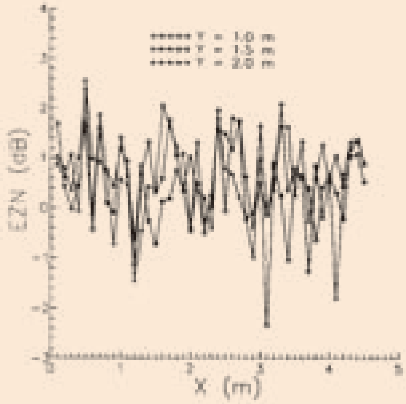

Fig. 5. Normalized electric field magnitude for various values of y. Other parameters: $f = 4$ GHz, $Q = 10^5$, and $x_0 = y_0 = 0.5$ m.

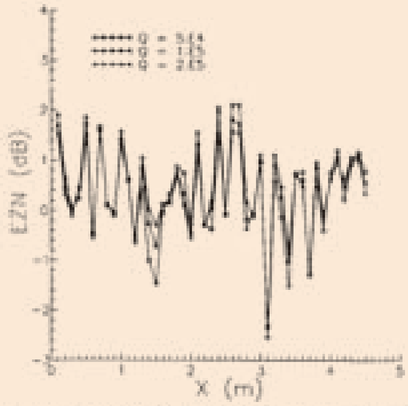

Fig. 6. Normalized electric field magnitude for various values of Q.

Fig. 7. Geometry for two line sources in a rectangular cavity.

V. Multiple-Source, Phase Stirring

For single-frequency, high-power excitation of reverberation chambers, multiple source antennas are advantageous because they eliminate the need for combining high-power signals [18]. A second possible benefit of multiple sources is improved field uniformity. In this section the case of two line sources is examined as shown in Fig. 7.

If the two sources are incoherent or if the relative phase of the two sources is averaged over 2π, radians, then square of the total field is the sum of the squares of the fields due to the two sources

$$|E_z|^2 = |E_{z0}|^2 + |E_{z1}|^2 \tag{30}$$

TABLE II
Average and Standard Deviation of the Field for Two Sources at a Single Frequency

x_1 (m)	y_1 (m)	r_{10}	Average (dB)	Stand. Dev. (dB)
3.5	0.6	0	-5.81	6.20
3.5	0.6	1000	-9.04	5.74
3.5	0.6	1	-7.13	3.89
0.5	2.5	1	-3.13	4.78
4.0	2.5	1	-2.03	5.65

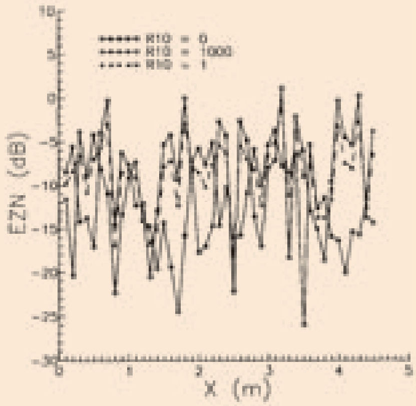

Fig. 8. Normalized electric field magnitude for two line sources of relative strength r_{10}.

where E_{z0} is the field produced by line source I_0 located at (x_0, y_0) and E_{z1} is the field produced by line source I_1 located at (x_1, y_1). For parametric studies, r_{10} is introduced as the ratio of the magnitude of I_1 to I_0:

$$|I_1| = r_{10}|I_0|. \tag{31}$$

In addition, a field normalization is defined somewhat differently from (29) because two line sources, but only a single frequency, are used

$$|E_{zn}|^2 = \frac{1}{D_n^2}|E_z|^2$$

where

$$D_n^2 = (1 + r_{10}^2)|I_0|^2\eta_0^2 Q/(4ab). \tag{32}$$

In Figs. 8 and 9, curves of field strength are shown as a function of x for various cases. The same cavity parameters ($a = 4.57$ m, $b = 3.05$ m, and $Q = 10^5$) are chosen. Other parameters are $f = 4$ GHz and $y = 1.5$ m. In Fig. 8, the source coordinates are: $x_0 = y_0 = 0.5$ m, $x_1 = 3.5$ m, and $y_1 = 0.6$ m. The $r_{10} = 0$ curve is that of a single source, and the $r_{10} = 1000$ curve is approximately that of a single source at (x_1, y_1). The $r_{10} = 1$ curve represents equal excitation, and it has somewhat less spatial variability. The average field values and the standard deviations for all the curves are shown in Table II.

In Fig. 9, the two sources are excited equally ($r_{10} = 1$), but the location of the I_1 source is varied. The two curves have similar statistics as shown in Table II. Other calculations have shown similar trends. The conclusion is that the use of

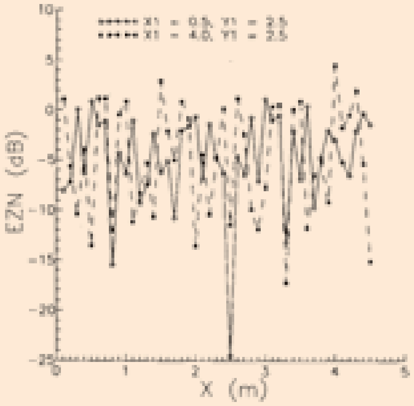

Fig. 9. Normalized electric field magnitude for two locations of the second line source I_1.

multiple sources at the same frequency is a useful method of injecting high power, but not very useful for improving field uniformity (about 1-dB improvement).

VI. Conclusion

A modal analysis and a uniform-field approximation have been presented for the fields in an idealized two-dimensional cavity. Even though the model is idealized, it allows a study of field uniformity produced by frequency stirring. The results in Section IV indicate that good field uniformity (standard deviation less than 1 dB) can be obtained with a bandwidth of about 10 MHz at a center frequency of 4 GHz. Since the number of cavity modes excited is proportional to the bandwidth times the center frequency, an even smaller bandwidth is required at higher frequencies. However, a larger bandwidth is required at lower frequencies, and this result will limit the low-frequency effectiveness of the technique.

The use of two sources of the same single frequency for exciting the cavity has also been analyzed. Although this is an effective way of providing high-power excitation without requiring a combiner, it does not provide much improvement in field uniformity even if the sources are incoherent or varied in relative phase. Some additional mechanical or frequency stirring is required to excite additional modes needed for field uniformity.

A number of extensions to this work would be desirable. The same type of analysis could be performed for a three-dimensional, rectangular cavity. This would match typical existing reverberation chambers and would allow the study of polarization effects. Even though mechanical stirrers are difficult to analyze, frequency stirring in cavities of separable geometry (such as rectangular) can be analyzed by a standard modal analysis (at least for simple sources). The question of the effect of the nonzero bandwidth in performing immunity measurements, particularly for test objects with sharp resonances, could be studied theoretically and experimentally. A final question is whether the frequency stirring method has any application in emissions measurements where there is no control over the spectrum of the test object.

References

[1] P. Corona, G. Latmiral, and E. Paolini, "Performance and analysis of a reverberating enclosure with variable geometry," *IEEE Trans. Electromagn. Compat.*, vol. EMC-22, pp. 2–5, 1980.
[2] B. H. Liu, D. C. Chang, and M. T. Ma, "Eigenmodes and the composite quality factor of a reverberating chamber," National Bureau of Standards, Tech. Note 1066, 1983.
[3] R. E. Richardson, "Mode-stirred chamber calibration factor, relaxation time, and scaling laws," *IEEE Trans. Instrum. Meas.*, vol. IM-34, pp. 573–580, 1985.
[4] M. L. Crawford and G. H. Koepke, "Design, evaluation, and use of a reverberation chamber for performing electromagnetic susceptibility/vulnerability measurements," National Bureau of Standards, Tech. Note 1092, 1986.
[5] D. A. Hill, M. L. Crawford, M. Kanda, and D. I. Wu, "Aperture coupling to a coaxial air line: theory and experiment," *IEEE Trans. Electromagn. Compat.*, vol. 35, pp. 69–74, 1993.
[6] D. I. Wu and D. C. Chang, "The effect of an electrically large stirrer in a mode-stirred chamber," *IEEE Trans. Electromagn. Compat.*, vol. 31, pp. 164–169, 1989.
[7] T. A. Loughry, "Frequency stirring: An alternate approach to mechanical mode-stirring for the conduct of electromagnetic susceptibility testing," Phillips Lab., Tech. Rep. PL-TR-91-1036, 1991.
[8] J. M. Dunn, "Local, high-frequency analysis of the fields in a mode-stirred chamber," *IEEE Trans. Electromagn. Compat.*, vol. 32, pp. 53–58, 1990.
[9] P. M. Morse and K. U. Ingard, *Theoretical Acoustics*. New York: McGraw-Hill, 1968, sec. 9.5.
[10] P. M. Morse and H. Feshbach, *Methods of Theoretical Physics*. New York: McGraw-Hill, 1953.
[11] J. D. Jackson, *Classical Electrodynamics*. New York: Wiley, 1975, sec. 8.8.
[12] E. Argence and T. Kahan, *Theory of Waveguides and Cavity Resonators*. New York: Hart, 1967, sec. 22.4.
[13] R. H. Price, H. T. Davis, R. H. Born, E. P. Wenaas, R. Achenbach, V. Gieri, R. Thomas, J. Alcala, J. Hanson, W. Haynes, C. McCrea, C. Montano, R. Peterson, B. Trautlein, and R. Umber, "Determination of the statistical distribution of electromagnetic field amplitudes in complex cavities," JAYCOR, Rep. 88JAL129, 1988.
[14] R. N. Ghose, *Microwave Circuit Theory and Analysis*. New York: McGraw-Hill, 1963, p. 410.
[15] R. F. Harrington, *Time-Harmonic Electromagnetic Fields*. New York: McGraw-Hill, 1961, sec. 1-12.
[16] M. L. Crawford, M. T. Ma, J. M. Ladbury, and B. F. Riddle, "Measurement and evaluation of a TEM/reverberating chamber," National Institute of Standards and Technology, Tech. Note 1342, 1990.
[17] M. Abramowitz and I. A. Stegun, *Handbook of Mathematical Functions*. Washington, DC: National Bureau of Standards, 1964.
[18] M. L. Crawford, National Institute of Standards and Technology, 325 Broadway, Boulder, CO 80303, private communication.

David A. Hill (M'72–SM'76–F'87) was born in Cleveland, OH, on April 21, 1942. He received the B.S.E.E. and M.S.E.E. degrees from Ohio University, Athens, in 1964 and 1966, respectively, and the Ph.D. degree in electrical engineering from Ohio State University, Columbus, in 1970.

Since 1970 he has been a member of the Boulder scientific community. From 1970 to 1971 he was a Visiting Fellow with the Cooperative Institute for Research in Environmental Sciences, where he worked on pulse propagation. From 1971 to 1982 he was with the Institute for Telecommunication Sciences, where he worked on theoretical problems in antennas and propagation. Since 1982 he has been in the Electromagnetic Fields Division of the National Institute of Standards and Technology, where he has been working on EMC/EMI and remote sensing problems. He is also a Professor Adjoint in the Department of Electrical and Computer Engineering of the University of Colorado, Boulder.

Dr. Hill is a member of URSI Commissions A, B, E, and F. He has served as an Associate Editor for the IEEE Transactions on Geoscience and Remote Sensing and the IEEE Transactions on Antennas and Propagation. EMC